


RESEARCH PAPER

Mind the gap (junction): cGMP induced by nitric oxide in cardiac myocytes originates from cardiac fibroblasts

Lukas Menges¹ | Christian Krawutschke¹ | Ernst-Martin Füchtbauer² |
Annette Füchtbauer² | Peter Sandner³ | Doris Koesling¹ | Michael Russwurm¹ 

¹Institute of Pharmacology and Toxicology, Ruhr-University Bochum, Bochum, Germany

²Department of Molecular Biology and Genetics, Molecular Cell and Developmental Biology Aarhus University, Aarhus C, Denmark

³Drug Discovery, Cardiovascular Research, Bayer AG, Pharmaceuticals, Wuppertal, Germany

Correspondence

Michael Russwurm, Institute of Pharmacology and Toxicology, Ruhr-University Bochum, Bochum 44780, Germany.
Email: michael.russwurm@ruhr-uni-bochum.de

Funding information

Kommission für Finanzautonomie und Ergänzungsmittel; Deutsche Forschungsgemeinschaft, Grant/Award Number: KO 1157/4-1

Background and Purpose: The intracellular signalling molecule cGMP, formed by NO-sensitive GC (NO-GC), has an established function in the vascular system. Despite numerous reports about NO-induced cGMP effects in the heart, the underlying cGMP signals are poorly characterized.

Experimental Approach: Therefore, we analysed cGMP signals in cardiac myocytes and fibroblasts isolated from knock-in mice expressing a FRET-based cGMP indicator.

Key Results: Whereas in cardiac myocytes, none of the known NO-GC-activating substances (NO, GC activators, and GC stimulators) increased cGMP even in the presence of PDE inhibitors, they induced substantial cGMP increases in cardiac fibroblasts. As cardiac myocytes and fibroblasts are electrically connected via gap junctions, we asked whether cGMP can take the same route. Indeed, in cardiomyocytes co-cultured on cardiac fibroblasts, NO-induced cGMP signals were detectable, and two groups of unrelated gap junction inhibitors abolished these signals.

Conclusion and Implication: We conclude that NO-induced cGMP formed in cardiac fibroblasts enters cardiac myocytes via gap junctions thereby turning cGMP into an intercellular signalling molecule. The findings shed new light on NO/cGMP signalling in the heart and will potentially broaden therapeutic opportunities for cardiac disease.

1 | INTRODUCTION

In addition to **cAMP**, **cGMP** has been reported to play an important role in the regulation of cardiac functions. However, in contrast to the relatively precise knowledge of the action of cAMP, the understanding of the cGMP-induced effects and the underlying molecular mechanisms are matter of debate (Farah, Michel, &

Balligand, 2018; Hofmann, 2018; Kuhn, 2009; Potter, Yoder, Flora, Antos, & Dickey, 2009).

Stimulation of cardiac cAMP signalling, for example, via **β -adrenoceptors**, causes inotropic and lusitropic effects via **PKA**-mediated phosphorylation of several proteins involved in excitation-contraction coupling. In analogy to the cAMP signalling cascade, the **cGMP-dependent protein kinase** occurs in cardiomyocytes, and phosphorylation of phospholamban in response to **CNP** has been reported (Frantz et al., 2013). In addition to the activation of cGMP-dependent protein kinase I, cGMP has been proposed to increase cAMP by inhibiting **PDE3** (Kirstein et al., 1995; Kojda & Kottenberg, 1999) or to decrease cAMP by activating **PDE2** (Levy, 2013; Vandecasteele, Verde,

Abbreviations: % CER, % change of emission ratio; 8MMX, 8-methoxymethyl-IBMX; Ang II, angiotensin II; ANP, atrial natriuretic peptide; BAY60, BAY60-7550; BNP, brain natriuretic peptide; CNP, C-type natriuretic peptide; ES cells, embryonic stem cells; GSNO, S-nitrosoglutathione; NO-GC, NO-sensitive GC; ROI, region of interest; α/β GlycA, 18- α/β -glycyrrhetic acid

This is an open access article under the terms of the Creative Commons Attribution-NonCommercial-NoDerivs License, which permits use and distribution in any medium, provided the original work is properly cited, the use is non-commercial and no modifications or adaptations are made.

© 2019 The Authors. British Journal of Pharmacology published by John Wiley & Sons Ltd on behalf of British Pharmacological Society

Rücker-Martin, Donzeau-Gouge, & Fischmeister, 2001). Generally, two GCs, that is, the **membrane-bound receptor-coupled GC** activated by the natriuretic peptides ANP, BNP, and CNP and the **NO-sensitive GC (NO-GC)** acting as receptor for NO, are considered to be able to increase cGMP in cardiac myocytes (Stangherlin et al., 2011). The functional consequences of increased levels of cGMP are not clear, for example, low amounts of NO have been reported to cause positive inotropic effects but higher NO amounts elicit negative ones (Kojda et al., 1996). In addition to the NO-GC stimulating properties, NO has been proposed to alter cardiac function independently of cGMP (Lima, Forrester, Hess, & Stampler, 2010).

In order to identify the cGMP-generating and -degrading players in cardiac cells, we analysed cGMP increases with a FRET-based cGMP indicator (Russwurm et al., 2007) expressed in knock-in mice. In adult cardiac myocytes, the natriuretic peptide CNP but not ANP increased cGMP. Unexpectedly, neither NO nor any of the newly discovered NO-GC activators or stimulators induced cGMP increases in adult cardiac myocytes from these mice even if applied with the **broad-band PDE-inhibitor IBMX**. In stark contrast, NO induced pronounced cGMP increases in cardiac fibroblasts. Gap junctions were shown to be responsible for intercellular communication between cardiomyocytes and fibroblasts. Indeed, in cardiomyocytes co-cultured on cardiac fibroblasts, NO now increased cGMP. As two different groups of gap junction inhibitors abolished these NO-induced cGMP responses, we conclude that cGMP formed in response to NO in cardiac fibroblasts is able to enter cardiac myocytes and to execute its biological functions there.

2 | METHODS

2.1 | Animals

Mice ubiquitously expressing the FRET-based cGMP indicator (cGi-500, Russwurm et al., 2007) under the CAG promotor were generated by targeting the Rosa26 locus using the Ai6 targeting vector (Madisen et al., 2010; Addgene #22798). The targeting construct was linearized with KpnI and electroporated into CJ7 embryonic stem (ES) cells derived from 129S1/Sv mice (Swiatek & Gridley, 1993) to create the conditional ROSA26^{tm18(cGi500)Emfu} allele. The constitutively active ROSA26^{tm18.1(cGi500)Emfu} allele was generated by removal of the loxP-flanked stop cassette containing the selection marker by transient expression of Cre recombinase in ES cells. Chimeric mice were generated by injection of the ES cells into B6D2F2 mouse blastocysts (Wertz & Füchtbauer, 1994). Chimeric males were bred with C57BL/6 females, and agouti offspring (indicating germ-line transmission of the manipulated 129S1/Sv ES cells) were analysed for the presence of the cGi-500 transgene by PCR. Further backcrossing was performed with C57/BL6 mice.

Generation of the mice was approved by the Danish agricultural ministry (#2012-15-2934-00213). According to Directive 2010/63/EU of the European Parliament on the protection of animals used for scientific purposes and the German *Tierschutzgesetz*, breeding of

What is already known

- NO-induced cGMP has been proposed to play an important role in the heart.
- The underlying cGMP signals in cardiomyocytes are poorly characterized.

What this study adds

- NO-induced cGMP is formed in cardiac fibroblasts but not in myocytes.
- cGMP formed in fibroblasts can enter cardiac myocytes via gap junctions.

What is the clinical significance

- Stimulators or activators of guanylyl cyclase are being clinically investigated for cardiac disease.
- Fibroblast-myocyte coupling explains how these drugs can have effects on cardiac myocytes.

genetically altered lines without a harmful phenotype and killing of animals solely for the use of organs or tissues are not considered “procedures” or “animal experiments” and do not require permission. The introduced genetic alteration leading to the expression of a fluorescent reporter was neither expected to result in a harmful phenotype nor unexpectedly did so. Housing, feeding, watering, and handling of the animals was performed according to the Directive 2010/63/EU and the German *Tierschutz-Versuchstierverordnung*. Mice were held in a conventional mouse facility at 22°C, 50–60% humidity in a 12-hr light/dark cycle with free access to standard rodent chow and tap water. Animals were exclusively used for preparation of primary cell cultures. To prepare the cultures as detailed below, adult (6–12 weeks old) animals of either sex were killed by CO₂ and subsequently decapitated.

2.2 | Preparation of cardiomyocytes

Cardiomyocytes were prepared from isolated hearts by modified Langendorff perfusion with Type 2 collagenase as described by O'Connell, Rodrigo, and Simpson (2007). In brief, heparin (1 ml, 20 U·ml⁻¹ in 0.9% NaCl) was injected into both ventricles of the dissected heart. After resection and aortic cannulation, the heart was perfused (flow rate 5 ml·min⁻¹, 5 min, 37°C) with DE buffer (113-mM NaCl, 4.7-mM KCl, 0.6-mM K₂HPO₄, 0.6-mM Na₂HPO₄, 1.2-mM MgSO₄, 12-mM NaHCO₃, 10-mM KHCO₃, 10-mM HEPES, pH 7.4, 10-mM 2,3-butanedione monoxime, 5.5-mM glucose, and 30-mM taurine in H₂O) in the Langendorff apparatus. Subsequently, the heart was perfused (flow rate 5 ml·min⁻¹, 18 min) with digestion buffer (150 U·ml⁻¹ of collagenase Type 2 [Worthington], 0.7 U·ml⁻¹ of protease [Sigma P5147], and 50-μM CaCl₂ in DE buffer) in a circulating manner. Afterwards, the heart was cut such that both ventricles were removed from the apparatus; the tissue was pulled apart in small pieces that were incubated (15 min, 37°C) in 12.5-ml POT buffer (163 U·ml⁻¹ of collagenase

2, 0.7 U·ml⁻¹ of protease, 50-μM CaCl₂, and 10 mg·ml⁻¹ of BSA in DE buffer) in a water bath under gently rocking conditions. The tissue- and cell-containing solution was passed through a filter (200 μm), and cells were collected by centrifugation (180 x g, 2 min). The resulting pellet was stepwise resuspended in calcium-containing DE buffer with increasing calcium concentrations (62, 212, 500, and 1,000 μM; 10 mg·ml⁻¹ of BSA, each) followed by centrifugation (180 x g, 2 min). After the fourth step, the pellet was resuspended in 1-ml plating medium (100 U·ml⁻¹ of penicillin–streptomycin [Gibco], 10-mM 2,3-butanedione monoxime, and 5% [V/V] FBS in MEM Gibco #11575), and 100 μl were transferred to the centre of coverslips (diameter 25 mm) coated with laminin (1 μg·cm⁻²) beforehand. After incubation (1 hr, 37°C, 2% CO₂), 2-ml culture medium (100 U·ml⁻¹ of penicillin–streptomycin, 0.1 mg·ml⁻¹ of BSA, 10-mM 2,3-butanedione monoxime, 10 μg·ml⁻¹ of insulin, 5.5 μg·ml⁻¹ of transferrin, and 6.7 ng·ml⁻¹ of sodium selenite in MEM) was added to each coverslip and aspirated after 2 hr. Subsequently, again 2-ml culture medium was added, and the cells were stored (2% CO₂, 37°C). After 2 days, cardiomyocytes were used for live cell imaging.

2.3 | Preparation of cardiac fibroblasts

Cardiac fibroblasts were prepared according to Duerschmid, Trial, Wang, Entman, and Haudek (2015). The heart without the atria was washed in ice-cold basic buffer (10 ml, 14 μg·ml⁻¹ of gentamicin, 14 μg·ml⁻¹ kanamycin, 11-mM HEPES, and 30-mM taurine in Krebs–Henseleit buffer [118-mM NaCl, 4.7-mM KCl, 2.5-mM CaCl₂, 1.2-mM MgSO₄, 7.5-mM glucose, bubbled for 30 min with carbogen, 25-mM NaHCO₃ added subsequently, pH 7.4]), minced (1–2 mm) in 1-ml basic buffer, and washed again three times in 1-ml basic buffer. For digestion, tissue pieces were transferred into 3-ml collagenase 3 buffer (11-mM HEPES, 1 mg·ml⁻¹ of collagenase 3 [Worthington 4183], 160 μg·ml⁻¹ of thermolysin [Sigma T7902], and 20 U·ml⁻¹ of DNase I [Sigma DN25] in HBSS Gibco #14025), and the sample was gently agitated (10 min, 37°C). The supernatant was carefully filtered (70 μm) in 15-ml ice-cold stop buffer (10% [V/V] FBS, 20 U·ml⁻¹ of DNase I in basis buffer) on ice. The digestion (in 3-ml collagenase 3 buffer) and filtering steps were repeated until the tissue was almost completely digested (usually 5–6 times). The resulting cells in the stop buffer were collected by centrifugation (10 min, 200 x g), and the pellet was resuspended in 10-ml stop buffer. After an additional centrifugation (10 min, 200 x g), cells were resuspended in 1-ml fibroblast medium (1% antibiotic/antimycotic Gibco #15240, 10% FBS in DMEM/F-12 Gibco #21331). After transfer of 100 μl of the cell suspension to the centre of coverslips, cells were incubated for at least 2 hr (5% CO₂, 37°C). Subsequently, 1-ml fibroblast medium was added to the coverslips, they were swung gently to remove non-sedimented cells, and the culture medium was aspirated. The fibroblasts were grown in fibroblast medium, and the medium was exchanged after 3–4 days. After reaching confluency (approximately 7 days), the cells were used for live cell imaging and RIA measurements.

2.4 | Co-culture of cardiac fibroblasts and cardiomyocytes

In order to be able to measure cGMP signals selectively in cardiomyocytes, cardiac fibroblasts were prepared from wild-type mice as described above. After reaching confluency, cardiomyocytes, prepared from the cGi-500 mice as described above, were plated directly on the cardiac fibroblasts. Before plating the cardiomyocytes, the fibroblast medium was replaced by plating medium. The resulting co-culture was grown in plating medium (2% CO₂, 37°C) and was used for live cell imaging after 2–4 days.

To prepare non-touching co-cultures, ibidi 2-well inserts were placed onto coverslips. Fibroblasts (from wild-type mice) were seeded into one well and the second well was coated with laminin as above. After ~7 days, cardiac myocytes (from cGi-500 mice) were seeded into the second well and the insert was removed 3 hr later which resulted in a 500-μm gap between the cell types. The cultures were grown for additional 2–4 days and used for live cell imaging as above.

2.5 | Preparation of dermal fibroblasts and smooth muscle cells

Dermal fibroblasts were prepared as described by Seluanov, Vaidya, and Gorbunova (2010). Smooth muscle cells were prepared from mouse aorta as described in Krawutschke, Koesling, and Russwurm (2015).

2.6 | cGMP recording by live cell imaging

Live cell imaging of intracellular cGMP was performed as described in Krawutschke et al. (2015). In short, coverslips with cardiac myocytes, fibroblasts, or co-cultures were mounted on an inverted fluorescence microscope (Zeiss Axiovert 200 with a 10× objective) and continuously superfused with PBS (137-mM NaCl, 10-mM Na₂HPO₄, 2.7-mM KCl, and 1.8-mM KH₂PO₄). Baseline was recorded for 2 min followed by addition of drugs as follows.

ANP (300 nM) and CNP (300 nM) as positive control were consecutively applied for 5 min, each, in the absence or presence of IBMX (100 μM) as indicated (Figures 1a and 4a). For concentrations–response curves, cells were stimulated with CNP or S-nitrosoglutathione (GSNO) as indicated followed by 5-min application of IBMX (100 μM) when indicated (Figures 1b, 2a, and 4b). To analyse PDEs involved, cells were pre-stimulated (5 min) with the indicated drugs followed by co-application (5 min) of the PDE inhibitors 8-methoxymethyl-IBMX (8MMX, 50 μM), **BAY60-7550** (BAY60, 100 nM), **cilostamide** (10 μM), **sildenafil** (1 μM in Figures 3b and 4c and 10 μM in Figure 1c), BAY73-6691 (10 μM) or IBMX (100 μM) as indicated (Figures 1c, 3b, and 4c). GSNO (10 μM, Figure 1d), the GC stimulator BAY60-2770 (10 μM), the GC stimulators/NO-sensitizers BAY41-2272 (10 μM), and BAY41-8543 (1 μM) in the absence or presence of GSNO (10 μM) as indicated were superfused for 5 min together with IBMX (100 μM) followed by CNP (5 min, 300 nM, with 100-μM IBMX) as positive control (Figures 1d and 3a).

To analyse the effect of **angiotensin II** (Ang II) on NO-stimulated cGMP, cells were superfused with Ca²⁺-containing PBS (PBS + 0.9-mM CaCl₂) pre-stimulated with GSNO (5 min, 10 nM) in the absence and presence of the PDE1 inhibitor 8MMX (50 μM) followed by addition of Ang II (5 min, 10 μM) as indicated (Figure 3c). Co-cultures (touching or non-touching) were consecutively stimulated (5 min)—in the absence or presence of the gap junction inhibitor **carbenoxolone** (100 μM, Sigma-Aldrich) as indicated—with GSNO (10 μM) and IBMX (100 μM) followed (5 min) by CNP (300 nM) and IBMX (Figure 5b). To analyse the effect of acute application of gap junction inhibitors on NO-induced signals, co-cultures were preincubated (5 min) with GSNO (10 μM) and IBMX (100 μM) followed by a 20-min co-application of the gap junction inhibitors carbenoxolone (100 μM), GAP26 (100 μM, Tocris), GAP27 (100 μM, Bachem), 18α- or 18β-glycyrrhetic acid (α/βGlycA, 10 μM, Sigma-Aldrich), scrambled versions of GAP26 and GAP27, sGAP26 (100 μM, CFVRSSVPHKDYI, Alpha Diagnostics), or sGAP27 (100 μM, REKIITSFIPT, Alpha Diagnostics), respectively, when indicated (Figure 5c,d).

Excitation at 431 nm was performed every 2.4 or 5.4 s (for the co-cultures) using a polychrome V (Till Photonics, Munich) for up to 1,000 ms (depending on fluorescence intensity). Cyan fluorescent protein and yellow fluorescent protein emissions were simultaneously recorded using a beam splitter (Optical Insights, equipped with a 505-nm dichroic mirror and 465/30- and 535/30-nm bandpass filters) and a CCD camera (Sensicam QE, pco imaging). Images were analysed using ImageJ (Rasband, 2018). After subtraction of a background image (recorded without cells), the cyan fluorescent protein images were pixel-wise divided by the corresponding yellow fluorescent protein images. Cells were selected as regions of interest (ROI), and the depicted % change of emission ratio (% CER) was calculated by normalizing the ratios within each ROI to the corresponding baseline ratio recorded within the first 1.5 min of the measurement or to the ratio recorded within the first depicted minute (Figures 3c and 5c,d). Values obtained from the ROIs of one coverslip were averaged. For quantification and statistical analysis, cGMP levels reached during the last minute of the respective intervals (baseline or stimulation, *vide supra*) were determined. Multiple measurements performed with cells from one animal were considered technical replicates, averaged, and treated as $N = 1$.

2.7 | Measurement of intracellular cGMP in RIAs

For analysis of cGMP, cardiac fibroblasts prepared as described above and cultured in 12-well plates (3.65-cm² growth area) were washed twice with PBS and allowed to equilibrate in PBS for 10 min (37°C). After preincubation in the absence and presence of IBMX as indicated (300 μM, 10 min, 37°C), cells were incubated in the absence and presence of GSNO (500 μM, 5 min, 37°C). Subsequently, the supernatants were removed, and the cells were lysed with 500-μl ice-cold 70% ethanol. Cells were scraped, and debris were removed by centrifugation (15 min, 4°C, 21,000× *g*). The supernatants and the pellets were dried under N₂ at 100°C. Subsequently, the protein content of the pellet

was determined with Pierce™ BCA Protein Assay Kit (Thermo Fischer Scientific), and cGMP was determined in the supernatants by RIA as described elsewhere (Brooker, Harper, Terasaki, & Moylan, 1979). RIAs and protein assays were performed in technical duplicates; for each preparation = animal, three wells assigned to each condition were averaged and treated as $N = 1$.

2.8 | Data and statistical analysis

The data and statistical analysis comply with the recommendations of the *British Journal of Pharmacology* on experimental design and analysis in pharmacology (Curtis et al., 2018). Blinding was not feasible because experiments were conducted by an individual experimenter who weighed, dissolved and diluted the substances himself. Coverslips were randomly assigned to the test conditions. Data shown are means ± SEM; for bar graphs and RIAs, individual values and means are depicted. Group sizes correspond to the number of animals and were designed to be equal. Some preparations did not yield enough coverslips to perform measurements under all planned conditions; in these cases, some randomly assigned condition(s) had to be skipped. N numbers corresponding to animals = preparations are given in the respective figure legends. Statistical analysis was performed using Prism 8 (Graphpad Software, San Diego, CA, USA), $P < .05$ was set as threshold for statistical significance.

To analyse whether ANP, NO, and GC stimulators or activators increase cGMP (Figures 1a,d, 3a, and 4a), mean values before (1–2 min) and after application of drug (6–7 min) were compared by one-tailed Wilcoxon matched pairs test because the values are normalized to the values before drug application. Concentration–response curves (Figures 1b, 2a, and 4b) were fitted to a four parameter logistic function by non-linear regression in Excel (Microsoft, Redmond, WA, USA). To analyse whether PDE inhibitors applied on top of CNP or GSNO stimulation increased cGMP (Figures 1c, 3b, and 4c), we aimed to perform a two-way repeated measures ANOVA (type of PDE inhibitor × before/after addition of PDE inhibitor). However, because repeated measures ANOVA cannot handle missing values, we had to analyse the data instead by fitting a mixed model as suggested by Prism. According to the manufacturer, the results can be interpreted like repeated measures ANOVA. Post hoc tests (Sidak's multiple comparisons test for the factor before/after addition of PDE inhibitor) were only performed when the mixed model indicated interaction ($P < .05$, type of PDE inhibitor × before/after addition of PDE inhibitor). To analyse whether Ang II (Figure 3c) or gap junction inhibitors (Figure 5c,d) were effective, mean cGMP levels reached under all conditions during the last minute of the experiments were analysed by ANOVA only if variances were not significantly different (Brown–Forsythe's test). Only if the F test indicated significance, Dunnet's multiple comparisons test against control (Figures 3c and 5c) or Sidak's multiple comparisons test against the respective scrambled peptide (Figure 5d) were performed.

Data obtained from the RIA (Figure 2b–d) were log transformed because the variability increased with the mean. One-way ANOVA

was performed only if Brown–Forsythe's test did not indicate variance inhomogeneity. Post hoc comparisons using Sidak's multiple comparisons test were performed if the *F* test indicated significance. To analyse whether carbenoxolone or culturing in a non-touching manner changes the number of GSNO-responsive cells (Figure 5b), the number of myocytes responding to GSNO and/or the control CNP were counted and the fraction of GSNO-responsive cells was calculated. The Kruskal–Wallis test was applied as the data were neither normally distributed nor log transformation was possible because of many zero values. Post hoc Dunn's multiple comparisons test against control was performed only if the Kruskal–Wallis test indicated significance.

2.9 | Nomenclature of targets and ligands

Key protein targets and ligands in this article are hyperlinked to corresponding entries in <http://www.guidetopharmacology.org>, the common portal for data from the IUPHAR/BPS Guide to PHARMACOLOGY (Harding et al., 2018), and are permanently archived in the Concise Guide to PHARMACOLOGY 2017/18 (Alexander et al., 2017).

3 | RESULTS

3.1 | Cardiac myocytes

First, we characterized cGMP responses of adult cardiomyocytes isolated from knock-in mice expressing a FRET-based cGMP indicator. Whereas ANP failed to elevate cGMP even in the presence of the broad-spectrum PDE inhibitor IBMX (Figure 1a), the natriuretic peptide CNP caused pronounced increases of cGMP that were further enhanced by IBMX (from 19% to 35% CER, Figure 1b). The concentration–response curves for CNP revealed EC_{50} values of ~ 60

and ~ 30 nM in the absence and presence of IBMX respectively (see Figure 1b). Besides this subtle leftward shift, IBMX increased the cGMP signals by $\sim 10\%$ to 15% CER at all CNP concentrations tested. Next, we examined the PDE isoforms degrading cGMP formed in response to CNP and tested a selection of PDE inhibitors. As can be seen in Figure 1c, the highly specific PDE inhibitors, cilostamide for PDE3 and BAY60 for PDE2, added to CNP (300 nM) increased cGMP signals by 6% and 4% CER respectively. The effects of cilostamide and BAY60 were additive (9% CER) but not as high as that of the broad-spectrum PDE inhibitor IBMX (12% CER). On the other hand, roles of PDE1, PDE5, and PDE9 can be ruled out as the PDE5 inhibitor sildenafil in a concentration (10 μ M) which also inhibits PDE1 (Lukowski et al., 2010) and the specific PDE9 inhibitor BAY73-6691 did not increase cGMP.

Next, we tested for NO–GC-generated cGMP in the adult cardiac myocytes. High concentrations of the NO-releasing compound GSNO (10 μ M) even in the presence of IBMX failed to increase cGMP (Figure 1d). As NO is scavenged by myoglobin in cardiac myocytes very effectively (Wykes & Garthwaite, 2004), we considered NO-independent activation of NO–GC. Within the last years, new compounds that activate NO–GC have been identified: The NO–GC stimulators sensitize the enzyme towards NO and stimulate NO independently whereas the NO–GC activators act by replacing the prosthetic haem in NO–GC, thereby activating haem-free NO–GC or NO–GC with oxidized haem. Accordingly, we applied two NO–GC stimulators (BAY41-2272 and BAY41-8543) together with NO or the NO–GC activator BAY60-2770 to cardiac myocytes with the broad-band PDE inhibitor IBMX being present in every sample (see Figure 1d). Again, neither of the combinations led to measurable cGMP signals whereas CNP with IBMX applied as a positive control clearly did. In sum, cGMP increases in response to activation of NO–GCs in adult cardiac myocytes were undetectable under the conditions applied.

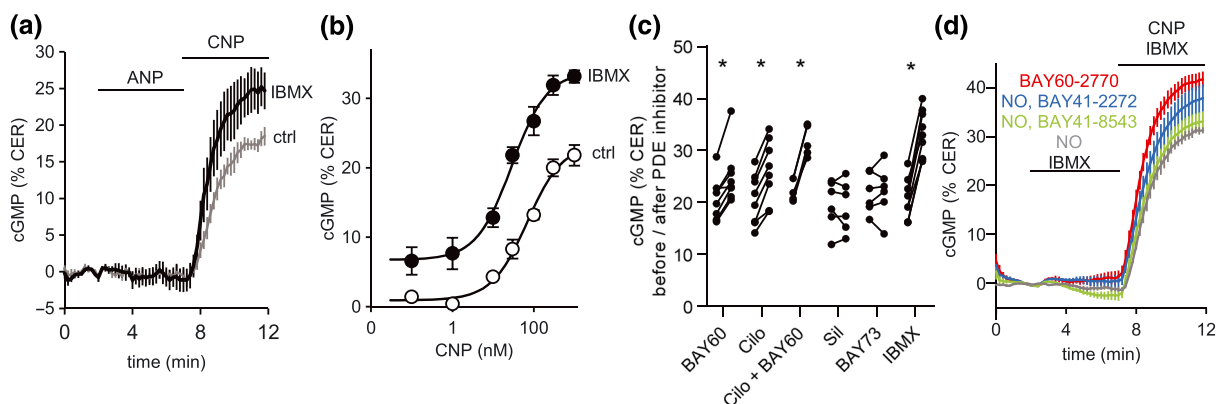


FIGURE 1 cGMP signals of adult primary cardiac myocytes. (a) In cardiac myocytes, ANP did not increase cGMP in the absence or presence of IBMX; CNP was applied as positive control. Values are means \pm SEM of myocytes from $N = 5$ mice. (b) CNP concentration–response curves were recorded with and without IBMX. Values are means \pm SEM of cardiac myocytes from $N = 5$ (10, 1,000 nM) or 6 (0.1, 1, 30–300 nM) mice. (c) Effect of PDE inhibitors added to CNP stimulation (300 nM). Shown are individual values (for each inhibitor, one pair corresponds to measurements from one mouse) before and after application of PDE inhibitors. $^*P < .05$, significant effect of PDE inhibitor. (d) Stimulation of cardiac myocytes by the indicated NO–GC-activating compounds does not increase cGMP; CNP was applied as positive control; all in the presence of IBMX. Data shown in the time courses as means \pm SEM of myocytes from $N = 5$ or $N = 6$ (BAY41-2272) mice. Cilo, cilostamide; Sil, sildenafil.

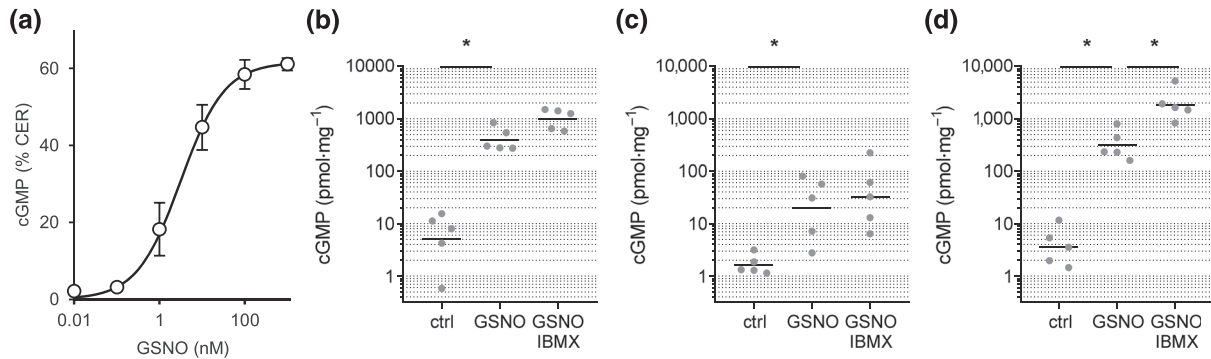


FIGURE 2 NO-induced cGMP of cardiac fibroblasts. (a) Primary cardiac fibroblasts were stimulated for 5 min with the indicated GSNO concentrations. Values are means \pm SEM of fibroblasts from $N = 5$ mice. (b–d) Cardiac (b) and dermal (c) fibroblasts and aortic smooth muscle cells (d) were stimulated with GSNO and IBMX as indicated and formed cGMP was determined by RIA. Data shown are individual values obtained from cells of one mouse each, together with means. * $P < .05$, significantly different as indicated.

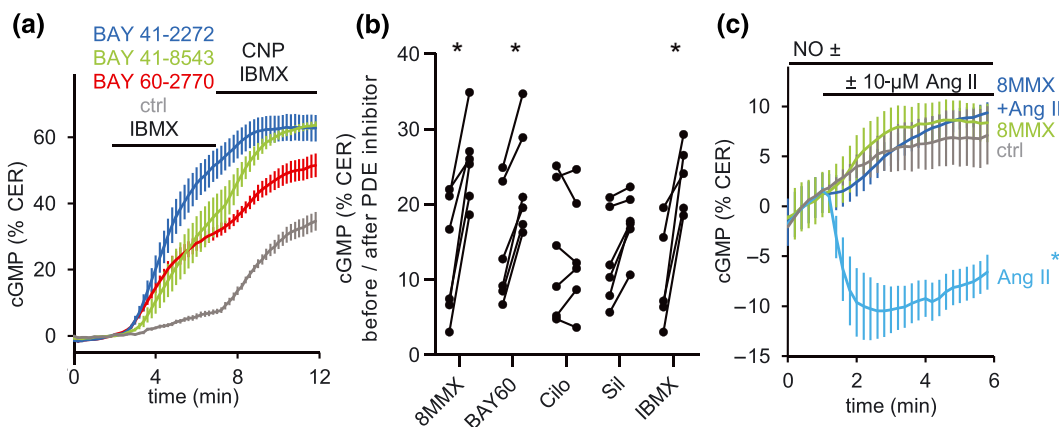


FIGURE 3 NO-GC-induced cGMP signals in cardiac fibroblasts. (a) Stimulation of cardiac fibroblasts by the indicated NO-GC-activating compounds increased cGMP. CNP was applied as positive control; all in the presence of IBMX. Data shown are the time courses as means \pm SEM of fibroblasts from $N = 5$ mice. (b) Effect of PDE inhibitors added to GSNO stimulation (1 nM). Data shown are individual values (for each inhibitor, one pair corresponds to measurements with fibroblasts from one mouse) before and after application of PDE inhibitors. * $P < .05$, significant effect of PDE inhibitor. Cilo, cilostamide; Sil, sildenafil. (c) Angiotensin II decreased GSNO-induced cGMP and the PDE1 inhibitor 8MMX abolished this effect. Data shown are means \pm SEM of fibroblasts from $N = 5$ (ctrl, 8MMX) or 6 (Ang II, Ang II + 8MMX) mice; * $P < .05$, significantly different from ctrl.

3.2 | Cardiac fibroblasts

Because on the one hand, we did not find NO-induced cGMP signals in cardiac myocytes, but on the other hand, substantial NO-stimulated cGMP-forming activity has been reported in heart homogenates (Arnold, Mittal, Katsuki, & Murad, 1977), we considered cardiac fibroblasts as source of the NO-stimulated cGMP-forming activity in the heart. Thus, we analysed cGMP signalling in cardiac fibroblasts and first determined the cGMP response towards GSNO. As shown in the concentration–response curve in Figure 2a, GSNO with an EC_{50} of ~ 3 nM very potently elicited marked increases in cGMP, of up to 60% CER, indicating saturation of the cGMP indicator. Thus, the NO-GC content in cardiac fibroblasts appeared to be very high; cGMP levels determined in RIAs revealed that the cGMP response induced by GSNO in fibroblasts was in a range similar to that measured in smooth muscle cells (400 vs. 300 pmol·mg⁻¹, Figure 2b,d respectively).

The pronounced NO-induced cGMP responses turned out to be a special feature of cardiac fibroblasts, as dermal fibroblasts displayed 20-fold lower cGMP levels (Figure 2c).

In accordance with a high NO-GC content in cardiac fibroblasts, the NO-GC activators and stimulators ineffective in cardiac myocytes elicited substantial cGMP increases of up to 50% CER, even in the absence of NO in cardiac fibroblasts (Figure 3a). This experiment also demonstrated (a) that the NO-GC activators and stimulators were effective and (b) that the applied method for detection of cGMP signals was suitable, thereby serving as a positive control for the undetectable NO-GC-generated cGMP in cardiac myocytes (see Figure 1d).

Characterization of the PDEs responsible for degradation of NO-induced cGMP (Figure 3b) revealed the contribution of PDE1 and PDE2. As a specific inhibitor for PDE1 is not commercially available, we used 8MMX (10 μ M) that inhibits PDE1 and PDE5 with a similar

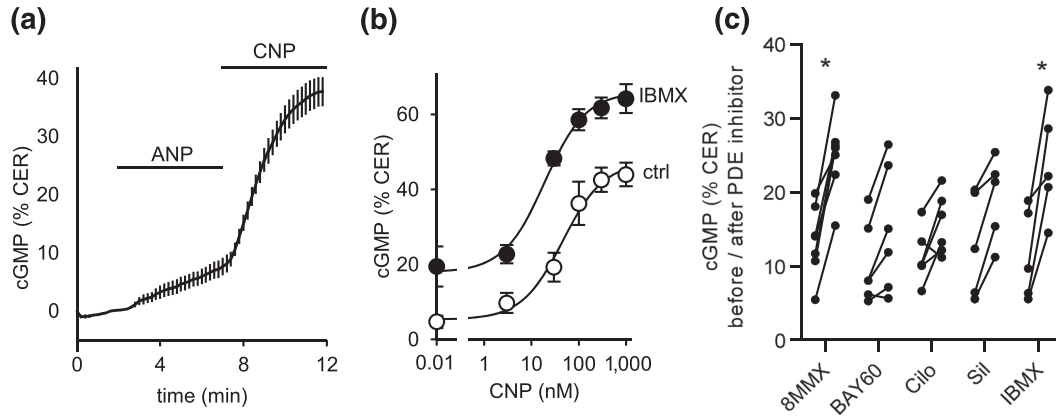


FIGURE 4 CNP-induced cGMP in cardiac fibroblasts. (a) ANP induced a small but significant increase of cGMP in cardiac fibroblasts; CNP was applied as positive control. Values are means \pm SEM of $N = 5$ mice. Data shown are the time courses as means \pm SEM of fibroblasts from $N = 7$ mice. (b) CNP concentration–response curves were recorded with and without IBMX. Values are means \pm SEM of fibroblasts from $N = 5$ mice. (c) Effect of PDE inhibitors added to CNP stimulation (3 nM). Data shown are individual values (for each inhibitor, one pair corresponds to measurements with fibroblasts from one mouse) before and after application of PDE inhibitors. * $P < .05$, significant effect of PDE inhibitor. Cilo, cilostamide; Sil, sildenafil.

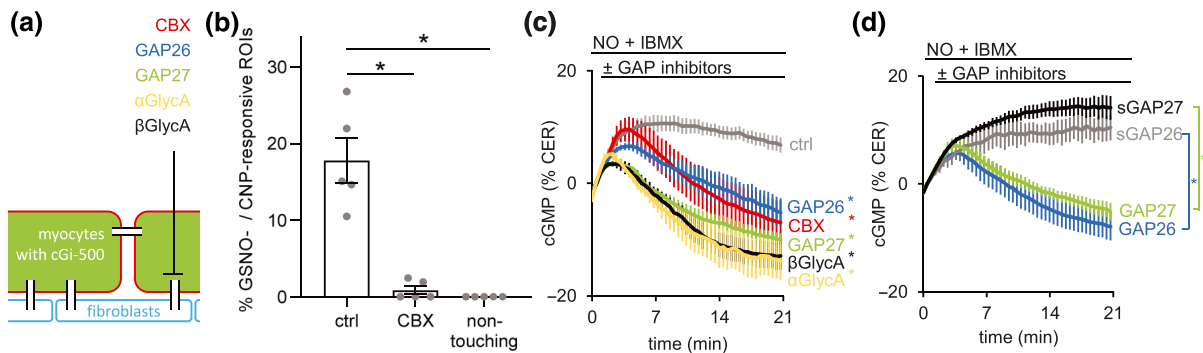


FIGURE 5 NO-induced cGMP signals in cardiac myocytes co-cultured with cardiac fibroblasts. (a) To detect cGMP specifically in cardiac myocytes, myocytes expressing the cGMP indicator cGi500 (indicated by green colour) were cultured on cardiac fibroblasts not expressing the indicator. (b) In the co-cultures, preincubation with the gap junction inhibitor carbenoxolone (CBX) or culturing myocytes and fibroblasts in a non-touching manner decreased the fraction of GSNO-responsive cardiac myocytes. Total number of viable myocytes was identified by subsequent CNP stimulation during the same recording. Shown are individual values together with means \pm SEM of co-cultures with myocytes of $N = 5$ mice; * $P < .05$, significantly different as indicated. (c) In the co-cultures, the indicated gap junction inhibitors decreased GSNO-induced cGMP. Values are normalized to the signal reached after 5 min preincubation with GSNO. Data shown are means \pm SEM of co-cultures with myocytes of $N = 7$ (ctrl), 6 (GAP26), or 5 (CBX, GAP27, and α/β GlycA) mice. * $P < .05$, significantly different from control. (d) In the co-cultures, GAP26 and GAP27 reversed NO-induced cGMP signals whereas the scrambled versions of the peptides, sGAP26 and sGAP27, were ineffective. Data shown are means \pm SEM of co-cultures with myocytes of $N = 5$ mice. * $P < .05$, significantly different from the respective scrambled peptide. α GlycA, 18- α -glycyrrhetic acid; β GlycA, 18- β -glycyrrhetic acid.

IC₅₀ (Ahn et al., 1997) and sildenafil at a concentration that inhibits only PDE5 (1 μ M). As 8MMX but not sildenafil increased NO-induced cGMP, we conclude that PDE1 is one of the major PDEs in cardiac fibroblasts. Considering the profound effect of PDE1 on NO-induced cGMP signals and the Ca²⁺ dependency of the enzyme, we considered effects of Ang II stimulation on NO-induced cGMP signals. Indeed, application of Ang II reversed the cGMP increases induced by NO (Figure 3c), which is compatible with enhanced cGMP hydrolysis due to PDE1 activation. In accordance with this course of action, the PDE1 inhibitor 8MMX abolished the cGMP-lowering effect of Ang II. Conceivably, Ang II by raising Ca²⁺ causes activation of PDE1 whose cGMP-degrading activity is then able to overcome the formation of cGMP induced by NO, resulting in a net fall in cGMP levels.

Whereas the natriuretic peptide ANP had only a marginal effect on cGMP in cardiac fibroblasts (Figure 4a), CNP caused a pronounced cGMP response in these cells. With ~40% CER, the maximal CNP-induced cGMP increase in cardiac fibroblasts (Figure 4b) was higher than in cardiomyocytes (~20% CER, see Figure 1b), and the EC₅₀ of ~30 nM was slightly lower than in cardiomyocytes (~60 nM). Application of PDE inhibitors, added to the CNP stimulation, revealed a major role of PDE1 for degradation of CNP-induced cGMP (Figure 4c). PDE2 inhibition had a much smaller effect than on NO-induced signals. Interestingly, PDE3 inhibition, which did not affect NO-induced signals, induced a slight and not statistically significant effect on CNP-induced signals, which may be an indicator of a membrane-associated PDE3 isoform.

3.3 | Co-cultured cardiac myocytes and fibroblasts

In the light of reported effects of NO on cardiac function and the substantial NO–GC-induced cGMP signals in fibroblasts in conjunction with their absence in cardiac myocytes, we tested the possibility that the NO–GC-generated cGMP could diffuse along the steep gradient into the cardiac myocyte, for example, via gap junctions connecting the two cell types.

To detect cGMP that had been generated in fibroblasts specifically in cardiac myocytes, we used a co-culture of cardiac fibroblasts not expressing the cGMP indicator with cardiac myocytes expressing the indicator (Figure 5a). In the co-culture, freshly isolated adult cardiac myocytes were plated on fibroblasts already grown for 1 week. After 2 to 4 days, the cGMP responses of the myocytes (with cGMP indicator) were continuously recorded as in the other experiments, and cultures were stimulated with GSNO (in the presence of IBMX) followed by CNP as positive control for viability of cardiac myocytes. Indeed, the addition of GSNO to the co-culture yielded cGMP increases in numerous cardiac myocytes amounting to 18% of the (viable) cardiac myocytes responding to CNP (Figure 5b). Parallel incubation of the co-culture with carbenoxolone, an inhibitor of gap junctions, prevented the GSNO-induced cGMP signals in cardiac myocytes. As control for the co-culture, cardiac fibroblasts (without indicator) and myocytes (expressing the indicator) were grown on the same coverslip side by side in a non-touching manner. Here, GSNO (in the presence of IBMX) failed to induce any cGMP signals, whereas the myocytes responded to CNP (see Figure 5b). We conclude the transfer of cGMP from fibroblasts to myocytes requires the physical interaction of the cells compatible with the formation of gap junctions.

Next, we asked whether carbenoxolone can affect the NO-induced cGMP signals instantaneously. In these experiments, the NO-induced cGMP response was triggered by GSNO and 5 min later, carbenoxolone was applied. As can be seen in Figure 5c, carbenoxolone abolished the NO-induced cGMP signals almost immediately indicating that gap junctions are required for the passage of cGMP formed in fibroblasts, into the cardiac myocyte. Any direct interaction of carbenoxolone with GSNO in analogy to the reaction of isoprenaline with NO (Rapoport, Waldman, Schwartz, Wink, & Murad, 1985) was ruled out in control experiments performed in fibroblasts (data not shown). Also, the additionally used gap junction inhibitors 18 α - and 18 β -glycyrrhetic acid reversed the NO-induced cGMP response. As further inhibitors of gap junctional communication, with a completely different structure from that of carbenoxolone or glycyrrhetic acid, we used connexin mimetic peptides. These short peptides corresponding to the first and second extracellular loop of **Connexin43 (Cx43)**, GAP26 and GAP27, have been used to disrupt the interaction between the connexins that form the gap junctions. Here, we used either peptide to inhibit the postulated gap junction-mediated cGMP increases in cardiac myocytes. As with carbenoxolone, GAP26 and GAP27 were applied 5 min after the induction of the cGMP response with GSNO. Both peptides greatly attenuated the NO-induced cGMP response (see Figure 5c). To ensure specificity of the observed effects of the connexin mimetic peptides,

GAP26 and GAP27 were additionally tested against their scrambled versions. As shown in Figure 5d, the scrambled versions sGAP26 and sGAP27 were not able to reverse the NO-induced cGMP response whereas the correct peptides did as before. In sum, the data support our conclusion of a gap junction-mediated transfer of cGMP from cardiac fibroblasts to cardiac myocytes.

4 | DISCUSSION

4.1 | Lack of NO-induced cGMP in cardiac myocytes

Whether cyclic GMP is formed in response to NO in cardiac myocytes has been a matter of debate (Castro, Schittl, & Fischmeister, 2010; Castro, Verde, Cooper, & Fischmeister, 2006; Stangherlin et al., 2011; Takimoto et al., 2005). Thus, we set out to analyse cGMP increases with the help of a FRET-based indicator in adult cardiac myocytes from mice. Similar experiments have been reported by the Nikolaev group (Götz et al., 2014). With the extremely sensitive indicator “red cGES-DE5” (Niino, Hotta, & Oka, 2009) expressed in cardiac myocytes of transgenic mice, the Nikolaev group found CNP to induce cGMP signals, whereas ANP and NO elicited cGMP signals only in the presence of IBMX that were barely distinguishable from the effect of IBMX alone. As **ODQ (1H-[1,2,4]oxadiazolo[4,3-a]quinoxalin-1-one)**, the inhibitor of NO–GC, abolished the IBMX-induced cGMP increase, they conclude that NO–GC was responsible for cGMP production under non-stimulated conditions and determined a cGMP concentration of approximately 10 nM (Götz et al., 2014). In our experimental setting, high amounts of GSNO, even in the presence of IBMX and GC stimulator compounds, did not raise the levels of cGMP. Similarly, the GC activator BAY60-2270 did not induce measurable cGMP increases under conditions of PDE inhibition. Thus, we conclude that NO–GC-formed cGMP in mouse cardiac myocytes is either locally restricted to regions not accessible to the indicator or remains below the detection limit. Using an olfactory **cyclic nucleotide-gated channel**, the Fischmeister group (Castro et al., 2006; Castro et al., 2010) was able to measure subsarcolemmal ANP and NO-induced cGMP in adult rat cardiomyocytes (for review, see Russwurm & Koesling, 2018). Whether this difference to our results was caused by species differences remains unresolved at this point. The affinity of our cGMP indicator cGi-500 (EC_{50} 500 nM) is clearly lower than that of “red cGES-DE5” (EC_{50} 40 nM), while the dynamic range, that is, change of emission ration is larger (70% vs. 20% CER in vitro; for review, see Russwurm & Koesling, 2018). As a result, substantial CNP-induced cGMP increases (in the presence of IBMX) were detected in cardiac myocytes with both indicators (14% and 35% CER with red cGES-DE5 and cGi-500, respectively) and the high potency of CNP was underpinned by the EC_{50} values in both studies (~30-nM CNP). PDE3 (6% CER) and PDE2 (4% CER) were identified as the major cGMP-degrading enzymes. ANP failed to increase cGMP in our study in contrast to a recent study of the Nikolaev group (Subramanian et al., 2018) in which ANP elicited ~2% ratio changes, specifically in T-tubules.

Previously, ANP-induced cGMP levels of 130–230 fmol per 10^5 cells were determined in RIAs (Götz et al., 2014; Klaiber et al., 2011). Using a cardiomyocyte volume of 20,000 fl per cell (Bensley, de Matteo, Harding, & Black, 2016; Schipke et al., 2014), this corresponds to intracellular cGMP concentrations of 70–135 nM. Those concentrations should be readily detectable by 10% CER with our cGMP indicator or lead to almost saturation of the sensitive “red cGES-DE5” indicator (Niino et al., 2009). It remains unresolved why neither we (see Figure 1a) nor Götz et al. (2014; fig. 2E 4% CER by IBMX + ANP, fig. 6B 4% CER by IBMX alone) were able to detect ANP-induced cGMP in the presence of IBMX. Furthermore, NO–GC-formed cGMP in primary cardiac myocyte cultures has also been assessed in RIA measurements and values of 6 and 3 pmol·mg⁻¹ of protein have been reported in the presence of NO–GC activating substances (NO donors, NO–GC stimulators, and activators; Kojda et al., 1996; Reinke et al., 2015). Considering the 100- to 400-fold higher NO-induced cGMP levels measured in cardiac fibroblasts (see Figure 4a), an almost negligible amount of fibroblasts present in the myocytes cultures, as regularly present (Kohl, 2003), would suffice to explain the reported values. Interestingly, despite the observed cGMP elevations, Reinke et al. (2015) excluded functional effects of NO–GC stimulators or activators on contractility of isolated myocytes.

4.2 | Pronounced NO-induced cGMP signals in cardiac fibroblasts

Cardiac myocytes make up the working portion of the heart. Nevertheless, there are other cells, for example, endothelial cells and smooth muscle cells and among those, fibroblasts are the most numerous in the heart, and active participation of fibroblasts in cardiac physiology and pathophysiology has already been demonstrated (see reviews in JMCC special issue: Sadoshima & Weiss, 2014). In addition to their structural roles, fibroblasts have been shown to interact with and to modulate the function of cardiac myocytes (Quinn et al., 2016). Thus, we analysed NO/cGMP signalling in cardiac fibroblasts and found that GSNO very potently (EC_{50} ~3 nM) induced marked cGMP increases (~60% CER), which saturated the indicator. In this context, it should be kept in mind that GSNO releases only fractional amounts of NO in the given time frame of 5 min (Gorren, Schrammel, Schmidt, & Mayer, 1996), and, thus, the half-effective NO concentration is far below 3 nM in accordance with the picomolar NO concentrations determined for NO–GC activation by the Garthwaite group (Batchelor et al., 2010). The high cGMP levels induced by NO were confirmed in RIAs, the values of 400-pmol cGMP per mg protein are comparable to those formed following NO-stimulation in smooth muscle cells (300 pmol per mg). The high NO responsiveness turned out to be a special feature of cardiac fibroblasts as dermal fibroblasts exhibited far lower cGMP levels (20-fold, see Figure 2c). In addition to NO–GC, cardiac fibroblasts also express **GC-B** as indicated by the CNP-induced cGMP increases which were even higher than the CNP-induced cGMP levels in cardiac myocytes. The minimal increase in cGMP induced by ANP argues for low expression levels of **GC-A** in cardiac fibroblasts, at least in mice.

Analysis of the cGMP-degrading enzymes revealed a major role for PDE1 in the degradation of NO- and CNP-induced cGMP. PDE2 had a considerable effect on NO-induced signals but contributed much less to the degradation of cGMP formed in response to CNP. Interestingly, PDE3 did not participate in the reversal of NO-induced cGMP increases but played a role in the degradation of CNP-induced cGMP. A similar finding, that is, a role of PDE3 in the degradation of GC-A-generated cGMP and the lack of an involvement in the hydrolysis of NO-induced cGMP, has also been described in vascular smooth muscle cells and argues for a greater effect of PDE3 on the cGMP that is formed closed to the membrane (Krawutschke et al., 2015).

We found Ang II to block the NO-induced cGMP response in fibroblasts and propose the Ca²⁺-induced activation of PDE1 as a possible mechanism underlining the functional antagonism between the renin-angiotensin and NO/cGMP systems. By their ability to proliferate, to transform into myofibroblasts, and to secrete extracellular matrix proteins like collagen, fibroblasts are known to be involved in cardiac remodelling processes. Conceivably, Ang II or other Ca²⁺-increasing substances counteract possible antiproliferative/antifibrotic actions of NO/cGMP via rapid stimulation of PDE1 in addition to the reported up-regulation of PDE1 on the mRNA and protein level in fibroblasts (Miller et al., 2011) and cardiomyocytes (Kim et al., 2001). In contrast to the latter study, we did not observe a relevant effect of PDE1 on cGMP in cardiac myocytes.

4.3 | NO-induced cGMP increases in cardiac myocytes co-cultured with fibroblasts

As inotropic and lusitropic effects of NO/cGMP have been described, we asked whether the high amounts of cGMP in cardiac fibroblasts were confined to this cell type or whether a molecular cell-connecting structure exists that allows cGMP to reach the cardiac myocyte. In addition to linking cardiac myocytes, gap junctions have been proposed to enable intercellular communication between myocytes and fibroblasts. The pore-forming gap junction channels consist of two hemichannels provided by either one of two neighbouring cells. Each hemichannel or connexon is a hexameric structure made up from six protein subunits, the connexins, which exist in multiple isoforms. Gap junction channels allow the propagation of electrical activity and the transfer of small molecules (up to 1,000 Da). With 1–5 hr, the $t_{1/2}$ of the channels is rather short, indicative of a high turnover (Darrow, Laing, Lampe, Saffitz, & Beyer, 1995; Fallon & Goodenough, 1981; Laird, 1996). Thus, we tested the possibility that gap junctions between cardiac myocytes and fibroblasts may be formed in a co-culture of both cell types. As it was our aim to specifically detect NO-induced cGMP signals in cardiac myocytes, we used cardiac myocytes expressing the FRET-based indicator cultured on fibroblasts without the indicator. Indeed, numerous cardiac myocytes in the co-culture, that is, 18% of CNP-responsive cardiac myocytes, exhibited GSNO-induced cGMP increases that were prevented by the gap junction inhibitor carbenoxolone. Carbenoxolone even instantaneously

interrupted NO-induced cGMP responses as its application onto co-cultures already treated with GSNO clearly reversed the cGMP increase, as did the additionally used gap inhibitors 18 α - and 18 β -glycyrrhetic acid. GAP26 and GAP27, short peptides corresponding to the first and second extracellular loop of Cx43, respectively, represent another structurally different group of gap junction inhibitors. Similar to carbenoxolone, 18 α - and 18 β -glycyrrhetic acid, the GAP26 and GAP27 peptides reversed NO-induced cGMP increases in cardiac myocytes whereas scrambled versions of the peptides applied as control did not.

Besides inhibiting the transfer of small molecules through gap junctions, the connexin mimetic peptides GAP26 and GAP27 have been shown to inhibit unapposed/non-junctional hemichannels of Cx43 (Wang et al., 2012). Typically, effects on hemichannels occur faster (within 3 min) than effects on gap junctions (Evans, Bultynck, & Leybaert, 2012), probably because the binding sites are more easily accessible in hemichannels. However, whereas a gap junction-mediated cGMP transfer obviously explains our data, an alternative hemichannel-dependent pathway to transduce a cGMP elevation in fibroblasts into the measured cGMP elevation in cardiac myocytes is difficult to imagine. Intriguingly, connexin-mimetic peptides have also been demonstrated to inhibit communication between cells and extracellular vesicles (exosomes). These connexin-carrying exosomes are proposed to carry intracellular signalling molecules thereby indirectly mediating intercellular communication over longer distances (Soares et al., 2015). Accordingly, exosome-mediated transfer of cGMP is expected to occur independently of physical connections between the donor and the acceptor cells. However, by non-touching co-cultures, physical contact between fibroblasts and myocytes was shown to be mandatory for the cGMP elevation in the cardiac myocytes in the present study, arguing against exosome-mediated communication as the underlying cause.

In sum, based on our observation that two groups of unrelated gap junction inhibitors abolished NO-induced cGMP increases in cardiac myocytes, we conclude that the cGMP formed in fibroblasts in response to NO is able to enter the cardiac myocytes via gap junctions and thereby provide the molecular basis for NO-induced cGMP effects in cardiac myocytes. In a previous report, gap junction-dependent diffusion of cGMP from mural granulosa cells to oocytes has been demonstrated and most interestingly, a hormone-induced change in gap junction permeability was described (Shuhaibar et al., 2015). Whether the permeability of gap junction-dependent diffusion of cGMP from the fibroblasts to the cardiac myocytes is also under control of hormones or intracellular signalling events has to be addressed in forthcoming studies. In a very recent publication, a beneficial effect of PDE2 inhibition in heart failure was shown to depend on cGMP formed by NO-GC, underlining the important function of the NO receptor in the heart (Baliga et al., 2018). Yet first and foremost, the presence of cGMP in cardiac myocytes as a result of NO-GC stimulation in fibroblasts has to be confirmed in whole heart preparations and then the way is paved for the identification of NO/cGMP effects in the working heart.

ACKNOWLEDGEMENTS

The authors gratefully acknowledge the technical assistance of Lisbeth Ahm Hansen, Lamija Kavazovic, and Ulla Krabbe. The contributions of Arkadius Pacha who started the cardiac myocyte preparation and of Caroline Vollmers who established the co-cultures are greatly appreciated. This work was supported by the Deutsche Forschungsgemeinschaft (DFG, Grant KO 1157/4-1) and the Kommission für Finanzautonomie und Ergänzungsmittel of the Medical Faculty (KOFFER).

AUTHOR CONTRIBUTIONS

M.R. and D.K. designed the project. L.M., C.K., and M.R. performed measurements and analysed the data. E.M.F. and A.F. generated the knock-in mouse. P.S. provided new reagents. L.M., C.K., P.S., D.K., and M.R. interpreted the data. D.K. and M.R. wrote and all authors edited the manuscript.

CONFLICT OF INTEREST

The authors declare no conflicts of interest. P.S. is a full-time employee of Bayer AG, Pharmaceuticals.

DECLARATION OF TRANSPARENCY AND SCIENTIFIC RIGOUR

This Declaration acknowledges that this paper adheres to the principles for transparent reporting and scientific rigour of preclinical research as stated in the *BJP* guidelines for [Design & Analysis](#), and [Animal Experimentation](#), and as recommended by funding agencies, publishers and other organisations engaged with supporting research.

ORCID

Michael Russwurm  <https://orcid.org/0000-0003-2947-9097>

REFERENCES

- Ahn, H. S., Bercovici, A., Boykow, G., Bronnenkant, A., Chackalamannil, S., Chow, J., ... Zhang, H. (1997). Potent tetracyclic guanine inhibitors of PDE1 and PDE5 cyclic guanosine monophosphate phosphodiesterases with oral antihypertensive activity. *Journal of Medicinal Chemistry*, *40*, 2196–2210. <https://doi.org/10.1021/jm9608467>
- Alexander, S. P. H., Fabbro, D., Kelly, E., Marrion, N. V., Peters, J. A., Faccenda, E., ... CGTP Collaborators (2017). The concise guide to PHARMACOLOGY 2017/18: Enzymes. *British Journal of Pharmacology*, *174*(Suppl 1), S272–S359. <https://doi.org/10.1111/bph.13877>
- Arnold, W. P., Mittal, C. K., Katsuki, S., & Murad, F. (1977). Nitric oxide activates guanylate cyclase and increases guanosine 3':5'-cyclic monophosphate levels in various tissue preparations. *Proceedings of the National Academy of Sciences of the United States of America*, *74*, 3203–3207. <https://doi.org/10.1073/pnas.74.8.3203>
- Baliga, R. S., Preedy, M. E. J., Dukinfield, M. S., Chu, S. M., Aubdool, A. A., Bubb, K. J., ... Hobbs, A. J. (2018). Phosphodiesterase 2 inhibition preferentially promotes NO/guanylyl cyclase/cGMP signaling to reverse the development of heart failure. *Proceedings of the National Academy of Sciences of the United States of America*, *115*, E7428–E7437. <https://doi.org/10.1073/pnas.1800996115>
- Batchelor, A. M., Bartus, K., Reynell, C., Constantinou, S., Halvey, E. J., Held, K. F., ... Garthwaite, J. (2010). Exquisite sensitivity to subsecond,

- picomolar nitric oxide transients conferred on cells by guanylyl cyclase-coupled receptors. *Proceedings of the National Academy of Sciences of the United States of America*, 107, 22060–22065. <https://doi.org/10.1073/pnas.1013147107>
- Bensley, J. G., de Matteo, R., Harding, R., & Black, M. J. (2016). Three-dimensional direct measurement of cardiomyocyte volume, nuclearity, and ploidy in thick histological sections. *Scientific Reports*, 6, 23756. <https://doi.org/10.1038/srep23756>
- Brooker, G., Harper, J. F., Terasaki, W. L., & Moylan, R. D. (1979). Radioimmunoassay of cyclic AMP and cyclic GMP. *Advances in Cyclic Nucleotide Research*, 10, 1–33.
- Castro, L. R. V., Schittl, J., & Fischmeister, R. (2010). Feedback control through cGMP-dependent protein kinase contributes to differential regulation and compartmentation of cGMP in rat cardiac myocytes. *Circulation Research*, 107, 1232–1240. <https://doi.org/10.1161/CIRCRESAHA.110.226712>
- Castro, L. R. V., Verde, I., Cooper, D. M. F., & Fischmeister, R. (2006). Cyclic guanosine monophosphate compartmentation in rat cardiac myocytes. *Circulation*, 113, 2221–2228. <https://doi.org/10.1161/CIRCULATIONAHA.105.599241>
- Curtis, M. J., Alexander, S., Cirino, G., Docherty, J. R., George, C. H., Giembycz, M. A., ... Ahluwalia, A. (2018). Experimental design and analysis and their reporting II. Updated and simplified guidance for authors and peer reviewers. *British Journal of Pharmacology*, 175, 987–993. <https://doi.org/10.1111/bph.14153>
- Darrow, B. J., Laing, J. G., Lampe, P. D., Saffitz, J. E., & Beyer, E. C. (1995). Expression of multiple connexins in cultured neonatal rat ventricular myocytes. *Circulation Research*, 76, 381–387. <https://doi.org/10.1161/01.RES.76.3.381>
- Duerschmid, C., Trial, J., Wang, Y., Entman, M. L., & Haudek, S. B. (2015). Tumor necrosis factor. A mechanistic link between angiotensin-II-induced cardiac inflammation and fibrosis. *Circulation. Heart Failure*, 8, 352–361. <https://doi.org/10.1161/CIRCHEARTFAILURE.114.001893>
- Evans, W. H., Bultynck, G., & Leybaert, L. (2012). Manipulating connexin communication channels. Use of peptidomimetics and the translational outputs. *The Journal of Membrane Biology*, 245, 437–449. <https://doi.org/10.1007/s00232-012-9488-5>
- Fallon, R. F., & Goodenough, D. A. (1981). Five-hour half-life of mouse liver gap-junction protein. *The Journal of Cell Biology*, 90, 521–526. <https://doi.org/10.1083/jcb.90.2.521>
- Farah, C., Michel, L. Y. M., & Balligand, J.-L. (2018). Nitric oxide signalling in cardiovascular health and disease. *Nature Reviews. Cardiology*, 15, 292–316. <https://doi.org/10.1038/nrcardio.2017.224>
- Frantz, S., Klaiber, M., Baba, H. A., Oberwinkler, H., Völker, K., Gaßner, B., ... Kuhn, M. (2013). Stress-dependent dilated cardiomyopathy in mice with cardiomyocyte-restricted inactivation of cyclic GMP-dependent protein kinase I. *European Heart Journal*, 34, 1233–1244. <https://doi.org/10.1093/eurheartj/ehr445>
- Gorren, A. C., Schrammel, A., Schmidt, K., & Mayer, B. (1996). Decomposition of S-nitrosoglutathione in the presence of copper ions and glutathione. *Archives of Biochemistry and Biophysics*, 330, 219–228. <https://doi.org/10.1006/abbi.1996.0247>
- Götz, K. R., Sprenger, J. U., Perera, R. K., Steinbrecher, J. H., Lehnart, S. E., Kuhn, M., ... Nikolaev, V. O. (2014). Transgenic mice for real-time visualization of cGMP in intact adult cardiomyocytes. *Circulation Research*, 114, 1235–1245. <https://doi.org/10.1161/CIRCRESAHA.114.302437>
- Harding, S. D., Sharman, J. L., Faccenda, E., Southan, C., Pawson, A. J., Ireland, S., ... NC-IUPHAR (2018). The IUPHAR/BPS guide to PHARMACOLOGY in 2018: Updates and expansion to encompass the new guide to IMMUNOPHARMACOLOGY. *Nucl Acids Res*, 46, D1091–D1106. <https://doi.org/10.1093/nar/gkx1121>
- Hofmann, F. (2018). A concise discussion of the regulatory role of cGMP kinase I in cardiac physiology and pathology. *Basic Research in Cardiology*, 113, 31. <https://doi.org/10.1007/s00395-018-0690-1>
- Kim, D., Rybalkin, S. D., Pi, X., Wang, Y., Zhang, C., Munzel, T., ... Yan, C. (2001). Upregulation of phosphodiesterase 1A1 expression is associated with the development of nitrate tolerance. *Circulation*, 104, 2338–2343. <https://doi.org/10.1161/hc4401.098432>
- Kirstein, M., Rivet-Bastide, M., Hatem, S., Bénardeau, A., Mercadier, J. J., & Fischmeister, R. (1995). Nitric oxide regulates the calcium current in isolated human atrial myocytes. *The Journal of Clinical Investigation*, 95, 794–802. <https://doi.org/10.1172/JCI117729>
- Klaiber, M., Dankworth, B., Kruse, M., Hartmann, M., Nikolaev, V. O., Yang, R.-B., ... Kuhn, M. (2011). A cardiac pathway of cyclic GMP-independent signaling of guanylyl cyclase A, the receptor for atrial natriuretic peptide. *Proceedings of the National Academy of Sciences of the United States of America*, 108, 18500–18505. <https://doi.org/10.1073/pnas.1103300108>
- Kohl, P. (2003). Heterogeneous cell coupling in the heart. An electrophysiological role for fibroblasts. *Circulation Research*, 93, 381–383. <https://doi.org/10.1161/01.RES.0000091364.90121.0C>
- Kojda, G., & Kottenberg, K. (1999). Regulation of basal myocardial function by NO. *Cardiovascular Research*, 41, 514–523. [https://doi.org/10.1016/S0008-6363\(98\)00314-9](https://doi.org/10.1016/S0008-6363(98)00314-9)
- Kojda, G., Kottenberg, K., Nix, P., Schlüter, K. D., Piper, H. M., & Noack, E. (1996). Low increase in cGMP induced by organic nitrates and nitrovasodilators improves contractile response of rat ventricular myocytes. *Circulation Research*, 78, 91–101. <https://doi.org/10.1161/01.RES.78.1.91>
- Krawutschke, C., Koesling, D., & Russwurm, M. (2015). Cyclic GMP in vascular relaxation. Export is of similar importance as degradation. *Arteriosclerosis, Thrombosis, and Vascular Biology*, 35, 2011–2019. <https://doi.org/10.1161/ATVBAHA.115.306133>
- Kuhn, M. (2009). Function and dysfunction of mammalian membrane guanylyl cyclase receptors. Lessons from genetic mouse models and implications for human diseases. *Handbook of Experimental Pharmacology*, (191), 47–69.
- Laird, D. W. (1996). The life cycle of a connexin. Gap junction formation, removal, and degradation. *Journal of Bioenergetics and Biomembranes*, 28, 311–318. <https://doi.org/10.1007/BF02110107>
- Levy, F. O. (2013). Cardiac PDEs and crosstalk between cAMP and cGMP signalling pathways in the regulation of contractility. *Naunyn-Schmiedeberg's Archives of Pharmacology*, 386, 665–670. <https://doi.org/10.1007/s00210-013-0874-z>
- Lima, B., Forrester, M. T., Hess, D. T., & Stamler, J. S. (2010). S-nitrosylation in cardiovascular signaling. *Circulation Research*, 106, 633–646. <https://doi.org/10.1161/CIRCRESAHA.109.207381>
- Lukowski, R., Rybalkin, S. D., Loga, F., Leiss, V., Beavo, J. A., & Hofmann, F. (2010). Cardiac hypertrophy is not amplified by deletion of cGMP-dependent protein kinase I in cardiomyocytes. *Proceedings of the National Academy of Sciences of the United States of America*, 107, 5646–5651. <https://doi.org/10.1073/pnas.1001360107>
- Madisen, L., Zwingman, T. A., Sunkin, S. M., Oh, S. W., Zariwala, H. A., Gu, H., ... Zeng, H. (2010). A robust and high-throughput Cre reporting and characterization system for the whole mouse brain. *Nature Neuroscience*, 13, 133–140. <https://doi.org/10.1038/nn.2467>
- Miller, C. L., Cai, Y., Oikawa, M., Thomas, T., Dostmann, W. R., Zaccolo, M., ... Yan, C. (2011). Cyclic nucleotide phosphodiesterase 1A. A key regulator of cardiac fibroblast activation and extracellular matrix remodeling

- in the heart. *Basic Research in Cardiology*, 106, 1023–1039. <https://doi.org/10.1007/s00395-011-0228-2>
- Niino, Y., Hotta, K., & Oka, K. (2009). Simultaneous live cell imaging using dual FRET sensors with a single excitation light. *PLoS ONE*, 4, e6036. <https://doi.org/10.1371/journal.pone.0006036>
- O'Connell, T. D., Rodrigo, M. C., & Simpson, P. C. (2007). Isolation and culture of adult mouse cardiac myocytes. *Methods in Molecular Biology*, 357, 271–296.
- Potter, L. R., Yoder, A. R., Flora, D. R., Antos, L. K., & Dickey, D. M. (2009). Natriuretic peptides. Their structures, receptors, physiologic functions and therapeutic applications. *Handbook of Experimental Pharmacology*, (191), 341–366.
- Quinn, T. A., Camelliti, P., Rog-Zielinska, E. A., Siedlecka, U., Poggioli, T., O'Toole, E. T., ... Kohl, P. (2016). Electrotonic coupling of excitable and nonexcitable cells in the heart revealed by optogenetics. *Proceedings of the National Academy of Sciences of the United States of America*, 113, 14852–14857. <https://doi.org/10.1073/pnas.1611184114>
- Rapoport, R. M., Waldman, S. A., Schwartz, K., Winquist, R. J., & Murad, F. (1985). Effects of atrial natriuretic factor, sodium nitroprusside, and acetylcholine on cyclic GMP levels and relaxation in rat aorta. *European Journal of Pharmacology*, 115, 219–229. [https://doi.org/10.1016/0014-2999\(85\)90694-6](https://doi.org/10.1016/0014-2999(85)90694-6)
- Rasband, W. S. (2018). *ImageJ*. Bethesda, Maryland, USA: National Institutes of Health. Retrieved from <http://imagej.nih.gov/ij/1997-2018>
- Reinke, Y., Gross, S., Eckerle, L. G., Hertrich, I., Busch, M., Busch, R., ... Felix, S. B. (2015). The soluble guanylate cyclase stimulator riociguat and the soluble guanylate cyclase activator cinaciguat exert no direct effects on contractility and relaxation of cardiac myocytes from normal rats. *European Journal of Pharmacology*, 767, 1–9. <https://doi.org/10.1016/j.ejphar.2015.09.022>
- Russwurm, M., & Koesling, D. (2018). Measurement of cGMP-generating and -degrading activities and cGMP levels in cells and tissues. Focus on FRET-based cGMP indicators. *Nitric Oxide*, 77, 44–52. <https://doi.org/10.1016/j.niox.2018.04.006>
- Russwurm, M., Mullershausen, F., Friebe, A., Jäger, R., Russwurm, C., & Koesling, D. (2007). Design of fluorescence resonance energy transfer (FRET)-based cGMP indicators: A systematic approach. *The Biochemical Journal*, 407, 69–77. <https://doi.org/10.1042/BJ20070348>
- Sadoshima, J., & Weiss, J. N. (2014). Cardiac fibroblasts. The good, the bad, the ugly, the beautiful. *Journal of Molecular and Cellular Cardiology*, 70, 1. <https://doi.org/10.1016/j.yjmcc.2014.03.009>
- Schipke, J., Banmann, E., Nikam, S., Voswinkel, R., Kohlstedt, K., Loot, A. E., ... Mühlfeld, C. (2014). The number of cardiac myocytes in the hypertrophic and hypotrophic left ventricle of the obese and calorie-restricted mouse heart. *Journal of Anatomy*, 225, 539–547. <https://doi.org/10.1111/joa.12236>
- Seluanov, A., Vaidya, A., & Gorbunova, V. (2010). Establishing primary adult fibroblast cultures from rodents. *Journal of Visualized Experiments : JoVE*, (44), pii: 2033. <https://doi.org/10.3791/2033>
- Shuhaibar, L. C., Egbert, J. R., Norris, R. P., Lampe, P. D., Nikolaev, V. O., Thunemann, M., ... Jaffe, L. A. (2015). Intercellular signaling via cyclic GMP diffusion through gap junctions restarts meiosis in mouse ovarian follicles. *Proceedings of the National Academy of Sciences of the United States of America*, 112, 5527–5532. <https://doi.org/10.1073/pnas.1423598112>
- Soares, A. R., Martins-Marques, T., Ribeiro-Rodrigues, T., Ferreira, J. V., Catarino, S., Pinho, M. J., ... Girao, H. (2015). Gap junctional protein Cx43 is involved in the communication between extracellular vesicles and mammalian cells. *Scientific Reports*, 5, 13243. <https://doi.org/10.1038/srep13243>
- Stangherlin, A., Gesellchen, F., Zoccarato, A., Terrin, A., Fields, L. A., Berrera, M., ... Zaccolo, M. (2011). cGMP signals modulate cAMP levels in a compartment-specific manner to regulate catecholamine-dependent signaling in cardiac myocytes. *Circulation Research*, 108, 929–939. <https://doi.org/10.1161/CIRCRESAHA.110.230698>
- Subramanian, H., Froese, A., Jönsson, P., Schmidt, H., Gorelik, J., & Nikolaev, V. O. (2018). Distinct submembrane localisation compartmentalises cardiac NPR1 and NPR2 signalling to cGMP. *Nature Communications*, 9, 2446. <https://doi.org/10.1038/s41467-018-04891-5>
- Swiatek, P. J., & Gridley, T. (1993). Perinatal lethality and defects in hind-brain development in mice homozygous for a targeted mutation of the zinc finger gene *Krox20*. *Genes & Development*, 7, 2071–2084. <https://doi.org/10.1101/gad.7.11.2071>
- Takimoto, E., Champion, H. C., Belardi, D., Moslehi, J., Mongillo, M., Mergia, E., ... Kass, D. A. (2005). cGMP catabolism by phosphodiesterase 5A regulates cardiac adrenergic stimulation by NOS3-dependent mechanism. *Circulation Research*, 96, 100–109. <https://doi.org/10.1161/01.RES.0000152262.22968.72>
- Vandecasteele, G., Verde, I., Rücker-Martin, C., Donzeau-Gouge, P., & Fischmeister, R. (2001). Cyclic GMP regulation of the L-type Ca(2+) channel current in human atrial myocytes. *Journal of Physiology (London)*, 533, 329–340. <https://doi.org/10.1111/j.1469-7793.2001.0329a.x>
- Wang, N., de Bock, M., Antoons, G., Gadicherla, A. K., Bol, M., Decrock, E., ... Leybaert, L. (2012). Connexin mimetic peptides inhibit Cx43 hemichannel opening triggered by voltage and intracellular Ca2+ elevation. *Basic Research in Cardiology*, 107, 304. <https://doi.org/10.1007/s00395-012-0304-2>
- Wertz, K., & Füchtbauer, E.-M. (1994). B6D2F1—An improved mouse hybrid strain for the production of ES cell germ line chimeras. *Transgene*, 1, 277–280.
- Wykes, V., & Garthwaite, J. (2004). Membrane-association and the sensitivity of guanylyl cyclase-coupled receptors to nitric oxide. *British Journal of Pharmacology*, 141, 1087–1090. <https://doi.org/10.1038/sj.bjp.0705745>

How to cite this article: Menges L, Krawutschke C, Füchtbauer E-M, et al. Mind the gap (junction): cGMP induced by nitric oxide in cardiac myocytes originates from cardiac fibroblasts. *Br J Pharmacol*. 2019;176:4696–4707. <https://doi.org/10.1111/bph.14835>